

Explainable Bayesian Optimization

Tanmay Chakraborty^{1,2}, Christin Seifert¹, Christian Wirth²

¹Philipps-Universität Marburg, Marburg, Germany

²Continental AG, Germany

tanmay.chakraborty@continental-corporation.com, christin.seifert@uni-marburg.de,
christian.2.wirth@continental-corporation.com

Abstract

In industry, Bayesian optimization (BO) is widely applied in the human-AI collaborative parameter tuning of cyber-physical systems. However, BO’s solutions may deviate from human experts’ actual goal due to approximation errors and simplified objectives, requiring subsequent tuning. The black-box nature of BO limits the collaborative tuning process because the expert does not trust the BO recommendations. Current explainable AI (XAI) methods are not tailored for optimization and thus fall short of addressing this gap. To bridge this gap, we propose TNTRules (TUNE-NOTUNE Rules), a post-hoc, rule-based explainability method that produces high quality explanations through multiobjective optimization. Our evaluation of benchmark optimization problems and real-world hyperparameter optimization tasks demonstrates TNTRules’ superiority over state-of-the-art XAI methods in generating high quality explanations. This work contributes to the intersection of BO and XAI, providing interpretable optimization techniques for real-world applications.

1 Introduction

The manual parameterization of cyber-physical systems is labor-intensive and heavily relies on domain experts, posing significant challenges in industrial settings [Neumann-Brosig *et al.*, 2019; Nagataki *et al.*, 2022]. Bayesian Optimization (BO), a model-based sequential optimization technique, has emerged as a solution, systematically exploring the parameter space to find an optimal setting [Shahriari *et al.*, 2015]. However, BO’s solution may not perfectly match the experts’ actual goal due to approximation errors and a simplified objective model, requiring human experts to tune parameters based on personal preferences and expert knowledge [Sundin *et al.*, 2022; Farrell and Peschka, 2020]. For example, using BO to set laser parameters involves using a simple laser simulator. However, the experts’ actual goal for the laser may differ from the BO results. Finally, the expert tunes the parameters based on their knowledge and BO’s recommendations.

The lack of interpretability in BO limits trust in BO recommendations among domain experts, similar to challenges in

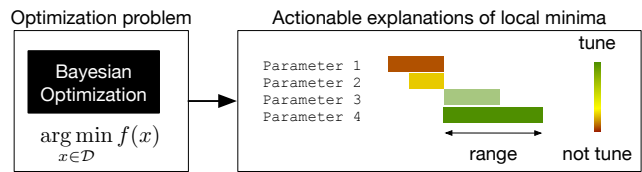


Figure 1: Explainable Bayesian Optimization with actionable explanations, showing parameter ranges and highlighting parameters that need tuning.

AI that led to the rise of explainable AI (XAI) [Rudin, 2022]. While various techniques have been developed to explain AI decisions, explanations for optimization algorithms are rare.

Explainable Bayesian optimization (XBO) should i) identify optimal solution, ii) provide insights into solution boundaries, and iii) identify and provide insights into potential alternative solutions (in the case of local minima).

Current XAI methods do not meet the aforementioned requirements i)-iii) of XBO. We address this gap by introducing TNTRules (Figure 1), a post-hoc rule-based explanation algorithm for BO. TNTRules offers local explanations through visual graphs and actionable rules, indicating which parameters should be adjusted or remain unchanged to improve results. For global explanations, TNTRules generates a ranked “IF-THEN” rule list. We rely on hierarchical agglomerative clustering (HAC) to uncover rules within the optimization space, including their associated uncertainties [Ran *et al.*, 2023]¹.

Unlike many XAI methods, TNTRules is controllable, allowing adjustments for high quality explanations or adapting to new use cases. We provide high quality explanations through multiobjective optimization, aiming to maximize explanation quality by tuning a threshold t_s , balancing various quality metrics.

Contributions

1. We present a method for explaining Bayesian Optimization as a set of global rules and local actionable explanations.
2. We introduce a novel variance based pruning technique for HAC to encode uncertainty.
3. We introduce a novel method based on multiobjective

¹Code: <https://github.com/tanmay-ty/TNTRules>

optimization to maximize the quality of explanations produced by TNTRules.

4. Our evaluation on hyperparameter optimization tasks shows that TNTRules outperforms other explanation methods. On common optimization test functions, we show TNTRules’ capability to identify the optimal region and its potential to detect other local minima.

2 Related Work

This section provides an overview of XAI, explanation presentations, and XAI method evaluation. Followed by rule-based explanations and optimizing the quality of explanations.

Explainable AI

XAI can be broadly classified into transparent models and post-hoc explanation methods, either specifically designed for certain model classes or applicable to a broad range of models (model agnostic) [Guidotti *et al.*, 2018]. Resulting explanations can be global, i.e., explain the full model, or local, i.e., explain a single sample. TNTRules generates a global surrogate model [Craven and Shavlik, 1995] as a rule set and local actionable rules.

Literature on **explaining optimization** is limited. The method of [Seitz, 2022] explains the core of BO, i.e., Gaussian Process (GP), primarily to produce feature rankings and uncertainty-aware feature rankings [Seitz, 2022], but they do not meet the XBO requirements i)-iii). RXBO, the closest work to ours, introduces a rule miner for optimization but does not deal with uncertainty while clustering and lacks multiple minima identification [Chakraborty *et al.*, 2024]. We use inspiration from the literature on rule-based surrogate models [Coppens *et al.*, 2019; Murdoch and Szlam, 2017; Amoukou and Brunel, 2022]. Those methods distill a base model into rule sets by leveraging a (probabilistic) surrogate model.

Explanation generation is usually tightly coupled to the **presentation format**. Following the model inspection pipeline of [Guidotti *et al.*, 2018], we argue that explanation generation and visualizations are distinct aspects, emphasizing the pivotal role of explanation presentation in enhancing understandability. TNTRules translates rules into visual explanations, following design patterns from commonly used visual-centric approaches like SHAP [Lundberg *et al.*, 2020] and LIME [Ribeiro *et al.*, 2016].

Similar to evaluations of machine learning models, explanation methods need to be evaluated. **XAI evaluation** libraries such as Quantus [Hedström *et al.*, 2023] are actively engaged in establishing evaluation benchmarks. A comprehensive study [Nauta *et al.*, 2023] identified 12 properties for evaluating XAI. We adopt a suitable subset of these characteristics to assess our TNTRules.

Rule Mining and Rule-based Explanations

Association rule mining has many established algorithms like Apriori, and Eclat [Yazgana and Kusakci, 2016]. XAI has adopted them for rule-based explanations because of their transparency, fidelity, and user-friendliness [van der Waa *et al.*, 2021]. We adopt a similar stance and select rules for

their high degree of comprehensibility. Similar to [Wang and Rudin, 2015], we present rules in descending order of utility.

Optimizing Quality of Explanations

Controllability, i.e., mechanisms for end users to steer the explanation method, is a desideratum for explanations [Nauta *et al.*, 2023]. Controlling an XAI method means being able to define and set parameters for an explanation method [Fernandes *et al.*, 2022]. Many XAI methods, like SHAP and LIME, lack control and assume their produced explanations are consistently optimal, rendering them black-boxes that explain black-boxes (the machine learning models). The existing body of literature on controllable XAI methods is limited. In a recent work [Pahde *et al.*, 2023], the concept of hyperparameter search for XAI has been introduced. Building upon this foundation, our contribution advances the field by proposing a novel approach to XAI hyperparameter search using multiobjective optimization.

3 Background and Problem Setting

This section briefly describes the background on Bayesian Optimization (BO) and Gaussian Processes (GPs) relevant for this paper, followed by the problem setting.

Bayesian Optimization, a sequential model-based optimization technique, uses a probabilistic model, usually a Gaussian Process (GP). BO uses uncertainty aware exploration/exploitation trade-offs, reducing the required number of iterations. [Pelikan *et al.*, 1999]

BO identifies minima for a black-box objective $f(\mathbf{x})$ defined in a bounded search-space $\mathcal{D} \subseteq \mathcal{R}^d$:

$$\mathbf{x}_{\text{opt}} = \arg \min_{\mathbf{x} \in \mathcal{D}} f(\mathbf{x}). \quad (1)$$

f is a black-box function that is *expensive to evaluate, noisy, and not known in closed-form*. The GP serves as an approximator of the objective function [Shahriari *et al.*, 2015]. We assume that the underlying GP approximates the optimization space sufficiently. Minimizing GP approximation error is a different research area [Rodemann and Augustin, 2022].

A **Gaussian Process** is a set of random variables with each finite set of those variables following a multivariate normal distribution. The distribution of a GP is the joint distribution of all variables. In GP, a distribution model is formulated around functions, each having a mean $m(\mathbf{x})$ and covariance function, commonly referred to as the kernel function $k(\mathbf{x}, \mathbf{x}')$. These collectively dictate the behavior of each function $f(\mathbf{x})$ at the specific location \mathbf{x} . When the mean is defined as $m(\mathbf{x}) = \mathbb{E}[f(\mathbf{x})]$, and the kernel function is articulated as $k(\mathbf{x}, \mathbf{x}') = \mathbb{E}[(f(\mathbf{x}) - m(\mathbf{x}))(f(\mathbf{x}') - m(\mathbf{x}'))]$, the GP framework is formally denoted as $f(\mathbf{x}) \sim GP(m(\mathbf{x}), k(\mathbf{x}, \mathbf{x}'))$. [Rasmussen and Williams, 2006]

Problem setting: In this work, we aim to explain the outcome of BO as approximated by its backbone GP. More formally: Given the function in Equation (1), the boundaries of the search space $\mathcal{D} = \{\mathbf{x} \in \mathcal{R}^d : lb^j \leq x^j \leq ub^j, \forall j \in \{1, \dots, d\}\}$, and the GP model, the goal is to enhance the interpretability of BO by identifying and describing the optimal

²3D loss landscape figure credited to: <https://github.com/tomgoldstein/loss-landscape>

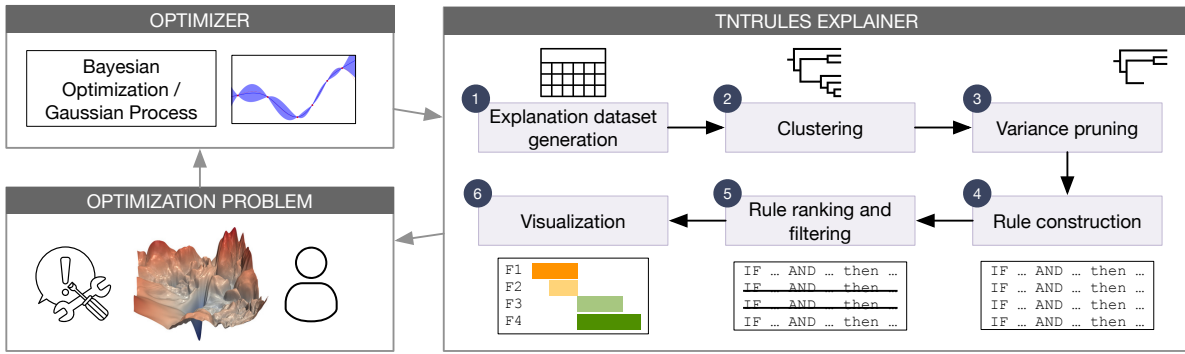


Figure 2: Given an optimization problem, TNTRules explains the optimizer by identifying parameter ranges for optimal areas in the search space. TNTRules first generates an explanation dataset (1) by sampling the search space. The dataset undergoes clustering (2); these clusters are pruned (3), and rules are constructed (4) for them. Subsequently, these rules are ranked and filtered (5), presenting the final set as explanations to the end user (6).²

areas of f as identified by BO. The explanation should be actionable, i.e., help users find promising settings for manual improvement of the solution. The explanation should identify and present i) the bounds for the best solution in a complicated optimization landscape and ii) the bounds for additional potential solutions together with their expected utility.

4 TNTRules

TNTRules (Figure 2) is our algorithm (Algorithm 1) for extracting and visualizing BO solution spaces. In TNTRules, we create an explanation dataset (1) for the objective function f , cluster it (2), and prune the cluster tree (3), then generate rules describing the clusters (4), rank and filter them for final explanations (5), and visualize the rules in a user-friendly manner (6) (cf. Figure 3). Additionally, TNTRules is optimized with multiobjective optimization to produce high-quality explanations (cf. Section 5).

4.1 Explanation Dataset Generation

In standard XAI settings, the explanation method has access to a data set. Usually, this is the training data, the ground-truth labels, and the model’s predictions. In the BO setting, the data set does not exist a-priori. BO dynamically acquires data during execution from the search space \mathcal{D} [Shahriari *et al.*, 2015]. The sampled data is small in quantity, biased towards optimal areas, and, thus, unsuitable.

Therefore, we generate an explanation dataset by uniformly sampling the search space for N_e samples $\mathbf{X}_e = \{x_1, \dots, x_{N_e}\} \sim \mathcal{U}(\mathcal{D})$. The GP is queried with \mathbf{X}_e to infer the posterior distribution characterized by vectors of mean $\boldsymbol{\mu}$ and standard deviation $\boldsymbol{\sigma}_y$. The resulting explanation dataset is formulated as $\mathbf{E} = [\mathbf{X}_e; \boldsymbol{\mu}; \boldsymbol{\sigma}_y]$.

4.2 Clustering

We use clustering to identify significant regions in the approximated posterior distribution (\mathbf{E}), considering the uncertainty within each region. We apply Hierarchical Agglomerative Clustering (HAC), an unsupervised, bottom-up clustering technique using the Ward criterion, to the explanation dataset \mathbf{E} [Murtagh and Legendre, 2011]. The resulting linkage matrix \mathbf{E}_{link} consists of links and distances between clusters.

Algorithm 1 TNTRules Algorithm

Require: BO search space: \mathcal{D} ,
 No. of explanation samples: N_e ,
 Clustering threshold: t_s
 Interestingness threshold: t_α
procedure *TNTRules*(\mathcal{D}, N_e, t_s)
 # Explanation dataset generation
 $\mathbf{X}_e \leftarrow \{x_1, \dots, x_{N_e}\} \sim \mathcal{U}(\mathcal{D})$
 $\boldsymbol{\mu}, \boldsymbol{\sigma}_y \leftarrow GP_{\text{predict}}(\mathbf{X}_e)$
 $\mathbf{E} \leftarrow [\mathbf{X}_e; \boldsymbol{\mu}; \boldsymbol{\sigma}_y]$
 # Clustering, Variance pruning, and Rule construction
 $\mathbf{E}_{\text{link}} \leftarrow Clustering(\mathbf{E})$
 $\mathbf{K} \leftarrow VariancePruning(\mathbf{E}_{\text{link}}, t_s)$
 $\rho_+, \rho_- \leftarrow RuleConstruction(\mathbf{E}, \mathbf{K})$
 # Rule ranking and filtering
for i **in** ρ_+ **do**
 $\rho_{temp}^i \leftarrow find(\mathbf{X}_e \in [\rho_-^i, \rho_+^i])$
 $Rel^i \leftarrow max(likelihood(GP_{\text{predict}}(\rho_{temp}^i)))$
 $Covr^i \leftarrow ECDF(\rho_+^i, \mathbf{X}_e)$
 $Supp^i \leftarrow ECDF([\rho_-^i, \rho_+^i], [\mathbf{X}_e; \boldsymbol{\mu}])$
 $Con^i \leftarrow Supp^i / Covr^i$
 $\alpha^i \leftarrow weightedSum(Rel^i, Covr^i, Supp^i, Con^i)$
end for
 $\rho \leftarrow FilterRules([\rho_-^i, \rho_+^i], \alpha, t_\alpha)$
return ρ
end procedure

\mathbf{E}_{link} is of size $(N_e - 1)$, where each row corresponds to a merge or linkage step in the clustering process. Pruning at different distances/levels of \mathbf{E}_{link} produces clusters with varying coverage [Salvador and Chan, 2004]. It is a challenge to determine the optimal threshold t_s or pruning distance for pruning that produces meaningful explanations, i.e., clusters that are both localized and cover areas around minima (cf. Section 6.2).

4.3 Variance Pruning

Instead of finding a threshold in the dendrogram like traditional methods to merge clusters, we use the HAC method to obtain only the linkage structure \mathbf{E}_{link} , then clusters are merged with the variance-based pruning mechanism captur-

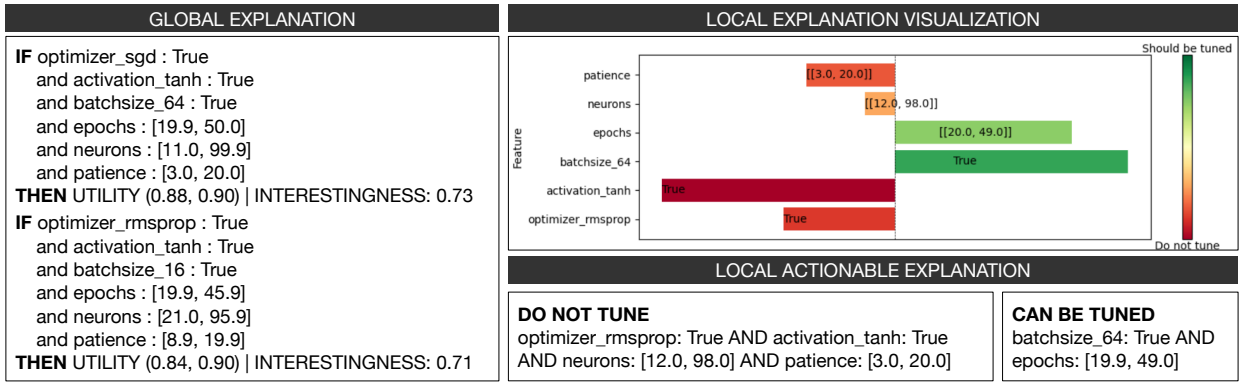


Figure 3: Visualizations from HPO use case with MLP model. Global explanations consist of 22 rules; here, we present two as examples. Local explanations include a sensitivity graph and actionable insights detailing which parameters to tune and what ranges.

ing data uncertainty. Pruning with conventional distance metrics fails to separate clusters when there is a high data variability and in the presence of outliers [Klutchnikoff *et al.*, 2022]. Our experiments show that a variance-based approach is most effective in such cases (cf. Section 7).

Let μ be the set of target values for the leaf nodes in the current subtree (the GP produces this value), n be the number of leaf nodes in the current subtree, and t_s is the predefined threshold for clustering. The condition for clustering is expressed as:

$$\left\{ \begin{array}{ll} \text{Merge leaf nodes} & \text{if } \text{Var}(\mu) \leq t_s \\ \text{Do not merge leaf nodes} & \text{if } \text{Var}(\mu) > t_s \end{array} \right.$$

$\text{Var}(\mu)$ represents the variance of the target values in μ . t_s is the predefined threshold for clustering and is a hyperparameter in our case.

4.4 Rule Construction

Based on the formed clusters \mathbf{K} , we extract the data points \mathbf{X}_e^i belonging to the subtree/cluster from \mathbf{X}_e to generate rules for each cluster. The antecedent’s rule bounds (ρ_{-}) are determined by taking the minimum and maximum over the extracted data points represented by each subtree. Similarly, for the consequent part (ρ_{+}), we calculate the confidence interval for the corresponding GP posterior, capturing the uncertainty: $\mu^i \pm 2 * \sigma_y^i$. A single rule looks like $[\min(X_e^i), \max(X_e^i)] \Rightarrow [\min(\mu^i - 2 * \sigma_y^i), \max(\mu^i + 2 * \sigma_y^i)]$. This step produces the full rule set denoted as ρ_{all} .

4.5 Rule Ranking and Filtering

The initial rule set ρ_{all} must be filtered and ranked based on their quality for producing the final explanations. We employ a quantitative framework to assess rule quality, focusing on localization within the optimization space and the ability to cover meaningful regions around potential solutions. Our evaluation integrates four metrics:

1. Coverage (*Covr*): how much a rule’s antecedent covers a region within the search space relative to the total area.
2. Support (*Supp*): evaluates the alignment of a rule’s domain with regions containing actual data.

3. Confidence (*Con*): is the ratio of Support to Coverage.
4. Relevance (*Rel*): is the maximum log-likelihood derived from the GP applied to the subset of data that conforms to a particular rule. Let \mathbf{I}_s denote the log-likelihood values for such instances, and \mathbf{I} represent the log-likelihoods of the entire dataset $Rel = \max_{\mathbf{I}_s \in \mathbf{I}}(\mathbf{I}_s)$ [Rasmussen and Williams, 2006, Chapter 2].

Coverage, Support, and Confidence are common in rule mining and computed using an empirical cumulative probability distribution [Witten *et al.*, 2017]. While effective in measuring the quality of the generated bounding boxes, they have limitations in locating optimal solution. We introduce the Relevance metric to address this limitation. Relevance effectively identifies regions where the GP is most likely to locate optimal solutions.

Finally, we define the overall Interestingness of a rule, bounded between (0,1], as the weighted sum: $\alpha = w_1 * Covr + w_2 * Supp + w_3 * Con + w_4 * Rel$, higher is better. The most interesting rules are presented by filtering the rule set ρ_{all} based on the Interestingness threshold t_α resulting in explanations ρ .

4.6 Visualization

TNTRules presents explanations ρ to the recipient through three visualization modes: global textual rules, local visual graphs, and local actionable explanations. The global explanations are expressed as an ordered list of “IF-THEN” rules, organized in decreasing order of Interestingness α (cf. Figure 3, left). Textual rules provide a simpler and interpretable model but are challenging to comprehend for an explanation recipient, especially in scenarios with long antecedents.

In Figure 3, local explanation visualizations appear on the right side. To generate these graphs, we conduct a sensitivity analysis of the GP model [Xu and Gertner, 2008], focusing on data samples covered by a rule. The sensitivity analysis identifies optimization model parameters that, when adjusted, may improve results. Tailored to the use case, we generate local actionable explanations. This representation abstracts non-essential rule components during tuning, enhancing user understanding. The graph and actionable explanations guide

the user by indicating parameters needing attention and those that can be ignored, simplifying interpretation, especially in cases with long antecedents. Aply, these rules are termed “TUNE-NOTUNE” rules.

5 Optimizing for Explanation Quality

We frame the challenge of providing good explanations as an optimization problem. We maximize the quality of explanations by leveraging the controllability property of TNTRules. We argue, that explanation quality depends on a trade-off between several metrics. We formulate this as multi-objective optimization, seeking an optimal t_s value that (cf. Section 4.2) concurrently maximizes Support, Relevance, and Rule set length (equivalent to minimizing Coverage of each rule): $t_{s_{opt}} = \arg \max_{t_s \in [0,1]} [Supp, Rel, |\rho|]$. The range between [0,1] is set because we normalize the variances in the data to be in [0,1].

We select these metrics to ensure explanations effectively identify solutions (Relevance) and provide precise localization with valid data support (Support and Rule set length).

Note that we can also frame this as a scalar optimization problem $t_{s_{opt}} = \arg \max_{t_s \in [0,1]} \alpha(t_s)$ with Interestingness α as the metric. In that case, the choice of weights for α becomes pivotal, as it involves balancing the various aspects of all metrics.

6 Experimental Setup

This section describes our evaluation metrics, threshold tuning, and experimental setup. For our experiments, we chose benchmark functions with ground truth and a common BO problem hyperparameter optimization (HPO) of machine learning models (where public data is available) [Snoek *et al.*, 2012].

6.1 Evaluation Metrics

We use the three-Cs evaluation metrics from the XAI literature for evaluating TNTRules [Nauta *et al.*, 2023].

Correctness: Measures the correctness of explanations concerning the model, i.e., Fidelity. Traditional Fidelity measures for decision boundaries are unsuitable for continuous distributions, so we use a sampling-based approach. Let N be the number of uniformly sampled points from rule antecedents. Define $F(x)$ as a function returning 1 for GP prediction of N_i lying within the rule consequent bounds and 0 otherwise. The mean fidelity, \bar{F} , is computed as $\bar{F} = \frac{1}{N} \sum_{i=1}^N F(x_i)$.

Compactness: Measures global rule set size ($|\rho|$) to determine how large the rule set is and that directly correlates to the effort needed to understand it.

Completeness: Evaluates to which extent the explanations cover all essential features for the use case. Specifically, we calculate the ratio of hyperparameters present in the longest rule of the explanations and the number of hyperparameters of the problem ($\frac{|\rho_{max}|}{|p|}$).

6.2 Optimizing Clustering Threshold (t_s)

To determine t_s , we use the pymoo [Blank and Deb, 2020] NSGA II [Deb *et al.*, 2002] implementation with 25 iterations. We select the solution with the highest rule set length out of the Pareto front.

6.3 Optimization Problems

We evaluate TNTRules on two sets of optimization problems: First, we benchmark using test functions for optimization, and second HPO with deep learning models. We set weights for interestingness α as $w_1 = 0.2, w_2 = 0.2, w_3 = 0.1, w_4 = 0.5$ for all experiments in this paper. We select these weights to give 50% importance to locating the solutions and the other 50% in creating the bounding boxes. Weight adjustments have not been explored in this paper. We conduct a comparative analysis of TNTRules with the XAI methods Decision rules (DR) [Apté and Weiss, 1997], RXBO [Chakraborty *et al.*, 2024], and RuleXAI [Macha *et al.*, 2022].

Optimisation Benchmark Functions

We evaluate TNTRules on five optimization benchmark functions [Mishra, 2006; Silagadze, 2007]. These domains allow to collect cheap groundtruth samples, enabling a direct evaluation. The selected functions and parameter values for TNTRules are in Appendix A Table 3.

Hyperparameter Optimisation Problems

We assess the performance of TNTRules in a practical deep learning context involving HPO tasks for both classification and regression problems. We utilized MNIST [Deng, 2012], CIFAR-10 [Krizhevsky *et al.*, 2009] and California Housing [Wu and others, 2020] dataset for the study. In these tasks, the number of minima is unknown from before; thus, selecting a threshold is difficult. We create the explanation dataset for TNTRules and use it as input for all methods. Fidelity of the methods is determined on GP samples, because groundtruth samples are too costly to obtain.

For TNTRules, we focus on rules with an Interestingness $\alpha > 0.7$, which are rules that have a greater chance of being an alternative solution. The parameter settings for TNTRules are given in Appendix A Table 3.

7 Results

This section presents results on the benchmark optimization functions, We also show through an ablation study that the GP approximation is a valid way of evaluating XBO, and finally, present results for the HPO use case. The results show TNTRules’ superiority over XAI baselines.

Optimisation Benchmark Functions

The visual results are given in Figure 4. On the left, all discovered rules ρ_{all} are depicted before filtering, with white boxes indicating their bounds. On the right, rules with $\alpha \geq 0.6$ (red boxes) and $0.6 > \alpha \geq 0.4$ (yellow boxes) are presented as highly and moderately interesting rules to the end user, respectively, after filtering. Rules with lower interestingness levels are omitted. The results indicate that TNTRules effectively localized high-interest minima identified by BO in four out of five cases, except for Himmelblau’s

		Ground Truth (iter = 1000)		Surrogate GP ($N_e = 1000$)	
		Compactness	Correctness	Compactness	Correctness
		$ \rho \downarrow$	$F \uparrow$	$ \rho \downarrow$	$F \uparrow$
BOOTH	DR	700 ± 0	0.88 ± 0.01	1000 ± 0	0.92 ± 0.01
	RXBO	10 ± 1	0.97 ± 0.01	5 ± 0	0.97 ± 0.01
	RuleXAI	16 ± 0	0.30 ± 0.00	12 ± 1	0.42 ± 0.01
	TNTRules	3 ± 2	1 ± 0.00	1 ± 0	0.98 ± 0.01
MATYAS	DR	700 ± 0	0.85 ± 0.02	1000 ± 0	0.90 ± 0.02
	RXBO	15 ± 0	0.98 ± 0.01	6 ± 5	0.97 ± 0.02
	RuleXAI	17 ± 1	0.27 ± 0.00	50 ± 2	0.48 ± 0.02
	TNTRules	6 ± 1	1 ± 0.00	1 ± 0	0.99 ± 0.00
HIMMEL.	DR	700 ± 0	0.83 ± 0.01	1000 ± 0	0.98 ± 0.01
	RXBO	30 ± 3	0.94 ± 0.03	25 ± 2	0.94 ± 0.01
	RuleXAI	17 ± 0	0.34 ± 0.01	35 ± 0	0.55 ± 0.01
	TNTRules	6 ± 2	0.99 ± 0.01	4 ± 1	0.99 ± 0.00
HOLDER.	DR	699 ± 1	0.88 ± 0.03	1000 ± 0	0.77 ± 0.03
	RXBO	14 ± 1	0.97 ± 0.02	12 ± 2	0.98 ± 0.01
	RuleXAI	17 ± 0	0.78 ± 0.00	55 ± 1	0.41 ± 0.02
	TNTRules	3 ± 2	0.98 ± 0.01	4 ± 0	0.98 ± 0.01
CROSS.	DR	700 ± 0	0.99 ± 0.00	1000 ± 0	0.97 ± 0.02
	RXBO	15 ± 5	0.99 ± 0.00	9 ± 3	0.99 ± 0.00
	RuleXAI	29 ± 1	0.96 ± 0.02	127 ± 1	0.99 ± 0.00
	TNTRules	4 ± 0	0.98 ± 0.00	4 ± 0	0.99 ± 0.00

Table 1: Results comparing XAI methods on Ground truth samples vs. GP surrogate. TNTRules outperformed, accurately identifying minima in the GP surrogate case and outperforming other methods in the ground truth case.

function, where the generated rule demonstrated moderate interestingness. The rule selection process reduced initially discovered rules by 98.5%, highlighting key rules as explanations. Rule curation resulted in a significant 98% reduction in the search space exploration during the re-execution of BO.

Ablation Study for BO Samples vs. GP Samples

In this paper, we assumed that the surrogate GP in BO sufficiently approximates direct BO evaluation of a function (ground truth (GT)) (cf. Section 3). Thus, we can evaluate on GP samples instead of GT samples, which is useful when obtaining GT samples is costly, as in HPO. As evaluating optimization test functions is cheap, we do an ablation study to demonstrate the consistency and independence of our results, regardless of whether we directly used GT or the surrogate GP with an explanation dataset.

We compared TNTRules with XAI methods under two settings: one with 1000 GT samples ($N_e = 0$) and the other with the sampled explanation dataset and the GP surrogate ($N_e = 1000$). For fidelity computation in the GT case, we held back 25% from the GT samples. In the GP-based evaluation, fidelity was computed using randomly generated 300 samples, as introduced in Section 6.1.

Table 1 presents results comparing GT samples and surrogate GP with an explanation dataset. TNTRules outperform all other methods under comparison, identifying all minima with high fidelity. RXBO performs second best, demonstrating better fidelity than decision rules and RuleXAI, suggesting good data approximation. Decision rules overfit, evident from numerous rules, while RuleXAI underfits, as reflected in low fidelity scores. An exception is the Cross-in-tray function, where all methods had high fidelity.

			Compactness	Completeness	Correctness
			$ \rho \downarrow$	$ \rho_{-1} _{max}/ p == 1.00$	$F \uparrow$
MLP (p = 6)	MNIST	DR	141 ± 5	4.33 ± 0.02	0.02 ± 0.01
		RXBO	62 ± 5	1.00 ± 0.00	0.80 ± 0.01
		RuleXAI	42 ± 1	1.33 ± 0.00	0.01 ± 0.00
		TNTRules	23 ± 1	1.00 ± 0.00	0.85 ± 0.01
MLP (p = 6)	HOUSING	DR	154 ± 6	2.50 ± 0.04	0.01 ± 0.00
		RXBO	34 ± 8	1.00 ± 0.00	0.61 ± 0.02
		RuleXAI	34 ± 1	1.50 ± 0.00	0.01 ± 0.00
		TNTRules	22 ± 1	1.00 ± 0.00	0.82 ± 0.03
RESNET (p = 6)	MNIST	DR	1000 ± 15	2.83 ± 0.02	0.93 ± 0.01
		RXBO	55 ± 2	1.00 ± 0.00	0.97 ± 0.01
		RuleXAI	117 ± 0	1.50 ± 0.00	0.86 ± 0.02
		TNTRules	3 ± 0	1.00 ± 0.00	1 ± 0.00
RESNET (p = 6)	CIFAR10	DR	1000 ± 13	1.66 ± 0.00	0.98 ± 0.01
		RXBO	57 ± 5	1.00 ± 0.00	0.99 ± 0.00
		RuleXAI	106 ± 0	2.00 ± 0.00	0.72 ± 0.01
		TNTRules	12 ± 0	1.00 ± 0.00	1 ± 0.00
XCCEPTIONNET (p = 11)	MNIST	DR	56 ± 2	0.54 ± 0.00	0.98 ± 0.01
		RXBO	69 ± 2	1.00 ± 0.00	0.99 ± 0.00
		RuleXAI	141 ± 1	0.72 ± 0.02	0.99 ± 0.00
		TNTRules	4 ± 0	1.00 ± 0.00	1 ± 0.00
XCCEPTIONNET (p = 11)	CIFAR10	DR	977 ± 3	2.27 ± 0.02	0.84 ± 0.02
		RXBO	21 ± 3	1.00 ± 0.00	0.80 ± 0.01
		RuleXAI	130 ± 0	0.72 ± 0.00	0.14 ± 0.01
		TNTRules	5 ± 1	1.00 ± 0.00	0.81 ± 0.05

Table 2: Comparing XAI methods with TNTRules for HPO with deep learning models. TNTRules outperforms all methods across all three criteria.

Hyperparameter Optimisation Problems

The results are presented in Table 2. TNTRules and RXBO consistently achieve a high correctness in their explanations, indicating a robust approximation of the underlying GP model. For compactness, the decision rules overfit the data, while RuleXAI and RXBO underfit the data, as observed from the number of rules they found. TNTRules consistently produced compact rules with high fidelity. The results here have the same trend as in the ablation study with test functions. Finally, RXBO and TNTRules exhibit completeness by associating each sample with a single, pruned explanation. In contrast to other methods that generate multiple shorter rules, lacking information for parameter tuning and violating completeness in this task. We can also observe that decision rules and RuleXAI have a long antecedent length (except XceptionNET MNIST where they were shorter than expected). This is because they repeat the same attribute in the antecedent with multiple ranges, increasing the overall length and complexity. From the results, TNTRules outperform the other XAI methods in qualitative and quantitative terms.

Ablation for Clustering Choices

We conducted an ablation study to support our design choices for HAC. We compared 16 combinations with seven HAC methods [Murtagh and Contreras, 2012], two distance metrics, distance pruning, and variance pruning. For benchmarking, we chose Himmelblau’s function with four known minima. The study evaluated the methods’ performance in identifying and localizing the four minima. HAC methods included Complete, Ward, Average, Median, Weighted, Centroid, and Single linkages, with Euclidean and Mahalanobis distances. Evaluation criteria included the number of initial rules, subset after applying the Interestingness filter ($\alpha > 0.6$), correct-

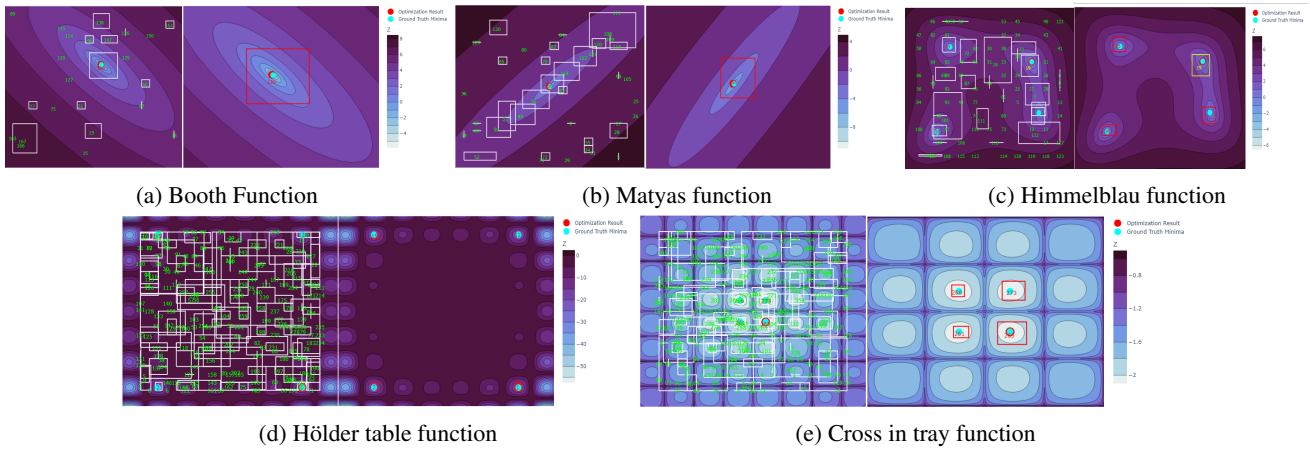


Figure 4: Results of the benchmark test functions marked with minima locations, red dot indicates BO found minima. Bounding boxes represent rule-based explanations. White boxes on the left show all rules from the HAC method. The final explanations are shown after filtering in right. Highly relevant rules are in red boxes, moderately relevant ones are in yellow boxes, and irrelevant ones are omitted.

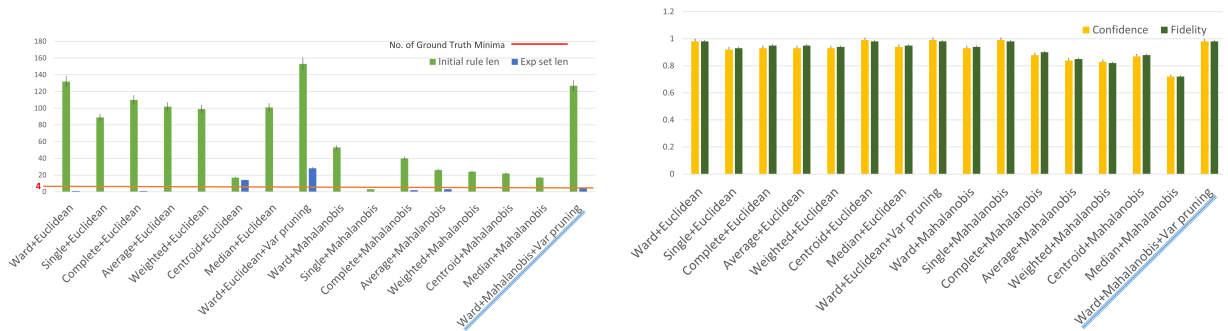


Figure 5: Ablation study comparing 16 HAC configurations. Left: number of initial rules discovered by each method compared to the resulting explanation set after applying the Interestingness filter ($\alpha > 0.6$). Right: rule set confidence and fidelity for each configuration. The optimal method is underlined.

ness, and overall confidence, as depicted in Figure 5.

From our ablation study, we note the effectiveness of using Ward linkage based on Mahalanobis distance and variance pruning, which accurately identifies all four solutions and provides tight bounding boxes. Ward and Complete linkages with Euclidean distance, along with distance-based pruning, yield one highly interesting rule ($\alpha > 0.6$) for one minima and three moderately interesting rules ($0.6 > \alpha \geq 0.4$) covering the remaining three minima. However, the dynamic threshold presents challenges when the number of minima is unknown. On the other hand, average linkage with Mahalanobis distance successfully identifies high-interest minima but results in larger bounding boxes, diminishing explanatory value as evident from the fewer rules found.

8 Conclusion

We have introduced and evaluated an explainable Bayesian optimization framework (XBO) called TNTRules. TNTRules generate high-fidelity localized rules within the optimization search space, effectively capturing the behavior of the underlying GP model in BO. It can identify alternative solutions, complementing BO results. The application of TNTRules

enables human-AI collaborative parameter tuning of cyber-physical systems through visualizations and tuning recommendations. Future work includes extending the framework to other probabilistic optimization methods and model-agnostic approaches.

A Appendix

Baseline Function	Known Minima	BO Iteration	Exp. samples N_e	threshold t_s
Booth function	1	100	200	$1e^{-1}$
Matyas function	1	100	200	$1e^{-3}$
Himmelblau function	4	200	400	$5e^{-2}$
Hölder table function	4	800	1600	$2e^{-3}$
Cross in tray Function	4	800	1600	$2e^{-6}$
MLP-MNIST	-	100	1000	0.8
MLP-Housing	-	100	1000	0.8
ResNET-MNIST	-	25	1000	0.7
ResNET-CIFAR10	-	25	1000	0.7
XceptionNET-MNIST	-	25	1000	0.5
XceptionNET-CIFAR10	-	25	1000	0.1

Table 3: Parameter settings for TNTRules, utilized for the two experiment sets (cf. Section 6.3)

Acknowledgments

This study was supported by BMBF Project hKI-Chemie: human-centric AI for the chemical industry, FKZ 01—S21023D, FKZ 01—S21023G and Continental AG.

References

- [Amoukou and Brunel, 2022] Salim I. Amoukou and Nicolas J.-B. Brunel. Consistent sufficient explanations and minimal local rules for explaining the decision of any classifier or regressor. In *Advances in Neural Information Processing Systems, NeurIPS*. Curran Associates, Inc., 2022.
- [Apté and Weiss, 1997] Chidanand Apté and Sholom Weiss. Data mining with decision trees and decision rules. *Future generation computer systems*, 13(2-3):197–210, 1997.
- [Blank and Deb, 2020] J. Blank and K. Deb. pymoo: Multi-objective optimization in python. *IEEE Access*, 8:89497–89509, 2020.
- [Chakraborty *et al.*, 2024] Tanmay Chakraborty, Christian Wirth, and Christin Seifert. *Post-hoc Rule Based Explanations for Black Box Bayesian Optimization*, volume CCIS, 1948 of *ECAI 2023 International Workshops*. Springer, Kraków, Poland, 2024.
- [Coppens *et al.*, 2019] Youri Coppens, Kyriakos Efthymiadis, Tom Lenaerts, Ann Nowé, Tim Miller, Rosina Weber, and Daniele Magazzeni. Distilling deep reinforcement learning policies in soft decision trees. In *Proceedings of the workshop on explainable artificial intelligence, IJCAI Workshop*, pages 1–6. IJCAI, 2019.
- [Craven and Shavlik, 1995] Mark Craven and Jude Shavlik. Extracting tree-structured representations of trained networks. *Advances in neural information processing systems*, 8, 1995.
- [Deb *et al.*, 2002] K. Deb, A. Pratap, S. Agarwal, and T. Meyarivan. A fast and elitist multiobjective genetic algorithm: Nsga-ii. *IEEE Transactions on Evolutionary Computation*, 6(2):182–197, 2002.
- [Deng, 2012] Li Deng. The mnist database of handwritten digit images for machine learning research. *IEEE Signal Processing Magazine*, 29(6):141–142, 2012.
- [Farrell and Peschka, 2020] Patricio Farrell and Dirk Peschka. Challenges in drift-diffusion semiconductor simulations. In Robert Klöfkorn, Eirik Keilegavlen, Florin A. Radu, and Jürgen Fuhrmann, editors, *Finite Volumes for Complex Applications IX - Methods, Theoretical Aspects, Examples*, pages 615–623, Cham, 2020. Springer International Publishing.
- [Fernandes *et al.*, 2022] Patrick Fernandes, Marcos Treviso, Danish Pruthi, André Martins, and Graham Neubig. Learning to scaffold: Optimizing model explanations for teaching. *Advances in Neural Information Processing Systems*, 35:36108–36122, 2022.
- [Guidotti *et al.*, 2018] Riccardo Guidotti, Anna Monreale, Salvatore Ruggieri, Franco Turini, Fosca Giannotti, and Dino Pedreschi. A survey of methods for explaining black box models. *ACM computing surveys (CSUR)*, 51(5):1–42, 2018.
- [Hedström *et al.*, 2023] Anna Hedström, Leander Weber, Daniel Krakowczyk, Dilyara Bareeva, Franz Motzkus, Wojciech Samek, Sebastian Lapuschkin, and Marina M-C Höhne. Quantus: An explainable ai toolkit for responsible evaluation of neural network explanations and beyond. *Journal of Machine Learning Research*, 24(34):1–11, 2023.
- [Klutchnikoff *et al.*, 2022] Nicolas Klutchnikoff, Audrey Poterie, and Laurent Rouvière. Statistical analysis of a hierarchical clustering algorithm with outliers. *Journal of Multivariate Analysis*, 192:105075, 2022.
- [Krizhevsky *et al.*, 2009] Alex Krizhevsky, Geoffrey Hinton, et al. Learning multiple layers of features from tiny images. 2009.
- [Lundberg *et al.*, 2020] Scott M. Lundberg, Gabriel G. Erion, Hugh Chen, Alex J. DeGrave, Jordan M. Prutkin, Bala Nair, Ronit Katz, Jonathan Himmelfarb, Nisha Bansal, and Su-In Lee. From local explanations to global understanding with explainable AI for trees. *Nat. Mach. Intell.*, 2(1):56–67, 2020.
- [Macha *et al.*, 2022] Dawid Macha, Michal Kozielski, Lukasz Wróbel, and Marek Sikora. Rulexai - A package for rule-based explanations of machine learning model. *SoftwareX*, 20:101209, 2022.
- [Mishra, 2006] Sudhanshu K Mishra. Some new test functions for global optimization and performance of repulsive particle swarm method. *Available at SSRN 926132*, 2006.
- [Murdoch and Szlam, 2017] W James Murdoch and Arthur Szlam. Automatic rule extraction from long short term memory networks. *arXiv preprint arXiv:1702.02540*, 2017.
- [Murtagh and Contreras, 2012] Fionn Murtagh and Pedro Contreras. Algorithms for hierarchical clustering: an overview. *Wiley Interdisciplinary Reviews: Data Mining and Knowledge Discovery*, 2(1):86–97, 2012.
- [Murtagh and Legendre, 2011] Fionn Murtagh and Pierre Legendre. Ward’s hierarchical clustering method: Clustering criterion and agglomerative algorithm. *CoRR*, abs/1111.6285, 2011.
- [Nagataki *et al.*, 2022] Masaki Nagataki, Keiichiro Kondo, Osamu Yamazaki, Kazuaki Yuki, and Yosuke Nakazawa. Online auto-tuning method in field-orientation-controlled induction motor driving inertial load. *IEEE Open Journal of Industry Applications*, 3:125–140, 2022.
- [Nauta *et al.*, 2023] Meike Nauta, Jan Trienes, Shreyasi Pathak, Elisa Nguyen, Michelle Peters, Yasmin Schmitt, Jörg Schlötterer, Maurice van Keulen, and Christin Seifert. From anecdotal evidence to quantitative evaluation methods: A systematic review on evaluating explainable ai. *ACM Comput. Surv.*, 2023.
- [Neumann-Brosig *et al.*, 2019] Matthias Neumann-Brosig, Alonso Marco, Dieter Schwarzmann, and Sebastian

- Trimpe. Data-efficient autotuning with bayesian optimization: An industrial control study. *IEEE Transactions on Control Systems Technology*, 28(3):730–740, 2019.
- [Pahde *et al.*, 2023] Frederik Pahde, Galip Ümit Yolcu, Alexander Binder, Wojciech Samek, and Sebastian Lapuschkin. Optimizing explanations by network canonization and hyperparameter search. In *Proceedings of the IEEE/CVF Conference on Computer Vision and Pattern Recognition*, pages 3818–3827, 2023.
- [Pelikan *et al.*, 1999] Martin Pelikan, David E Goldberg, Erick Cantú-Paz, et al. Boa: The bayesian optimization algorithm. In *Proceedings of the genetic and evolutionary computation conference GECCO-99*, volume 1. Citeseer, 1999.
- [Ran *et al.*, 2023] Xingcheng Ran, Yue Xi, Yonggang Lu, Xiangwen Wang, and Zhenyu Lu. Comprehensive survey on hierarchical clustering algorithms and the recent developments. *Artificial Intelligence Review*, 56(8):8219–8264, 2023.
- [Rasmussen and Williams, 2006] Carl Edward Rasmussen and Christopher K. I. Williams. *Gaussian processes for machine learning*. Adaptive computation and machine learning. MIT Press, 2006.
- [Ribeiro *et al.*, 2016] Marco Túlio Ribeiro, Sameer Singh, and Carlos Guestrin. "why should I trust you?": Explaining the predictions of any classifier. In *Proceedings of the International Conference on Knowledge Discovery and Data Mining, SIGKDD*, pages 1135–1144. ACM, 2016.
- [Rodemann and Augustin, 2022] Julian Rodemann and Thomas Augustin. Accounting for gaussian process imprecision in bayesian optimization. In *International Symposium on Integrated Uncertainty in Knowledge Modelling and Decision Making*, pages 92–104. Springer, 2022.
- [Rudin, 2022] Cynthia Rudin. Why black box machine learning should be avoided for high-stakes decisions, in brief. *Nature Reviews Methods Primers*, 2(1):81, 2022.
- [Salvador and Chan, 2004] Stan Salvador and Philip Chan. Determining the number of clusters/segments in hierarchical clustering/segmentation algorithms. In *16th IEEE international conference on tools with artificial intelligence*, pages 576–584. IEEE, 2004.
- [Seitz, 2022] Sarem Seitz. Gradient-based explanations for gaussian process regression and classification models. *arXiv preprint arXiv:2205.12797*, 2022.
- [Shahriari *et al.*, 2015] Bobak Shahriari, Kevin Swersky, Ziyu Wang, Ryan P Adams, and Nando De Freitas. Taking the human out of the loop: A review of bayesian optimization. *Proceedings of the IEEE*, 104(1):148–175, 2015.
- [Silagadze, 2007] ZK Silagadze. Finding two-dimensional peaks. *physics of Particles and Nuclei Letters*, 4:73–80, 2007.
- [Snoek *et al.*, 2012] Jasper Snoek, Hugo Larochelle, and Ryan P Adams. Practical bayesian optimization of machine learning algorithms. *Advances in neural information processing systems*, 25, 2012.
- [Sundin *et al.*, 2022] Iris Sundin, Alexey Voronov, Haoping Xiao, Kostas Papadopoulos, Esben Jannik Bjerrum, Markus Heinonen, Atanas Patronov, Samuel Kaski, and Ola Engkvist. Human-in-the-loop assisted de novo molecular design. *Journal of Cheminformatics*, 14(1):1–16, 2022.
- [van der Waa *et al.*, 2021] Jasper van der Waa, Elisabeth Nieuwburg, Anita H. M. Cremers, and Mark A. Neerincx. Evaluating XAI: A comparison of rule-based and example-based explanations. *Artif. Intell.*, 291:103404, 2021.
- [Wang and Rudin, 2015] Fulton Wang and Cynthia Rudin. Falling rule lists. In *Artificial intelligence and statistics*, pages 1013–1022. PMLR, 2015.
- [Witten *et al.*, 2017] Ian H. Witten, Eibe Frank, Mark A. Hall, and Christopher J. Pal. Chapter 3 - output: Knowledge representation. In *Data Mining (Fourth Edition)*, pages 67–89. Morgan Kaufmann, fourth edition, 2017.
- [Wu and others, 2020] Zixu Wu et al. Prediction of california house price based on multiple linear regression. *Academic Journal of Engineering and Technology Science*, 3(7.0), 2020.
- [Xu and Gertner, 2008] Chonggang Xu and George Zdzislaw Gertner. Uncertainty and sensitivity analysis for models with correlated parameters. *Reliability Engineering & System Safety*, 93(10):1563–1573, 2008.
- [Yazgana and Kusakci, 2016] Pinar Yazgana and Ali Osman Kusakci. A literature survey on association rule mining algorithms. *Southeast Europe Journal of soft computing*, 5(1), 2016.